

# Kerman-Onishi conditions in self-consistent tilted-axis-cranking mean-field calculations

Yue Shi (石跃),<sup>1,2</sup> C. L. Zhang (张春莉),<sup>1,3</sup> J. Dobaczewski,<sup>4,5</sup> and W. Nazarewicz<sup>1,6,4</sup>

<sup>1</sup>*Department of Physics and Astronomy, University of Tennessee, Knoxville, Tennessee 37996, USA*

<sup>2</sup>*Joint Institute for Heavy Ion Research, Oak Ridge National Laboratory, Oak Ridge, Tennessee 37831, USA*

<sup>3</sup>*State Key Laboratory of Nuclear Physics and Technology,  
School of Physics, Peking University, Beijing 100871, China*

<sup>4</sup>*Institute of Theoretical Physics, Faculty of Physics,  
University of Warsaw, ul. Hoża 69, PL-00681 Warsaw, Poland*

<sup>5</sup>*Department of Physics, PO Box 35 (YFL), FI-40014 University of Jyväskylä, Finland*

<sup>6</sup>*Physics Division, Oak Ridge National Laboratory, Oak Ridge, Tennessee 37831, USA*

**Background:** For cranked mean-field calculations with arbitrarily oriented rotational frequency vector  $\omega$  in the intrinsic frame, one has to employ constraints on average values of the quadrupole-moment tensor, so as to keep the nucleus in the principal-axis reference frame. Kerman and Onishi [Nucl. Phys. A **361**, 179 (1981)] have shown that the Lagrange multipliers that correspond to the required constraints are proportional to  $\omega \times \mathbf{J}$ , where  $\mathbf{J}$  is the average angular momentum vector.

**Purpose:** We study the validity and consequences of the Kerman-Onishi conditions in the context of self-consistent tilted-axis-cranking (TAC) mean-field calculations.

**Methods:** We perform self-consistent two-dimensional-cranking calculations (with and without pairing) utilizing the symmetry-unrestricted solver HFODD. At each tilting angle, we compare the calculated values of quadrupole-moment-tensor Lagrange multipliers and  $\omega \times \mathbf{J}$ .

**Results:** We show that in self-consistent calculations, the Kerman-Onishi conditions are obeyed with high precision. Small deviations seen in the calculations with pairing can be attributed to the truncation of the quasiparticle spectrum. We also provide results of systematic TAC calculations for triaxial strongly deformed bands in <sup>160</sup>Yb.

**Conclusions:** For non-stationary TAC solutions, Kerman-Onishi conditions link the non-zero values of the angle between rotational-frequency and angular-momentum vectors to the constraints on off-diagonal components of the quadrupole-moment tensor. To stabilize the convergence of self-consistent iterations, such constraints have to be taken into account. Only then one can determine the Routhian surfaces as functions of the tilting angles.

PACS numbers: 21.60.Jz, 21.10.Re, 21.10.Ky, 27.70.+q

## I. INTRODUCTION

Axially deformed nucleus can execute collective rotations with the angular momentum built along the axis that is perpendicular to the symmetry axis [1, 2]. Due to the larger moment of inertia, rotation about this axis is energetically more efficient in generating the same amount of angular momentum, compared to the mechanism of particle-hole excitations or non-collective rotations [3]. The standard theoretical framework to describe high-spin phenomena is the cranking model, in which a cranking term,  $-\omega_1 J_1$  [1, 2, 4], is added to the mean-field Hamiltonian.

In principle, a triaxial nucleus can rotate about an axis that does not coincide with the principal axis (PA) [5, 6]. The evidence for such rotations has been very limited, however, mainly owing to very indirect experimental information concerning triaxial shapes. Theoretical challenges include (i) the fact that very few nuclei are predicted to be triaxial in their ground states [7], and predictions are very model dependent [8]; (ii) triaxial minima in potential-energy surfaces associated with triaxial shapes are soft, and (iii) minima of Routhians in function of the tilting angles are shallow [9, 10], meaning the rotational axis can easily change its direction. The latter two chal-

lenges require the mean-field models to be able to handle various correlations in a self-consistent manner.

In self-consistent Hartree-Fock (HF) TAC calculations, when the rotational axis moves away from the PA, the nucleus has to stay fixed in the PA system. This can be realized by adding linear constraints that would guarantee that the resulting off-diagonal components of the inertia tensor vanish. In Ref. [11], Kerman and Onishi have shown that the corresponding Lagrange multipliers depend on the angular momentum, rotational frequency, and the quadrupole moments of the system through relation (3.6) in Ref. [11], referred to as the Kerman-Onishi (KO) conditions in the following. Subsequent applications seldom included such linear constraints, except for those described in Refs. [11–13], in which nuclear mean fields were either modeled by phenomenological potentials or the self-consistent fields of the pairing-plus-quadrupole Hamiltonian [13]. In this paper we extend these studies to mean-field approaches based on realistic energy density functionals (EDFs).

Recently, a multitude of high-spin bands in nuclei around <sup>158</sup>Er have been observed [14–20] and interpreted in terms of triaxial strongly deformed (TSD) structures predicted by the PA cranking (PAC) calculations [14, 21–24]. Specifically, in <sup>158</sup>Er, two minima (dubbed TSD1

and TSD2) with similar  $\beta_2$  and  $|\gamma|$  deformations, but opposite signs of  $\gamma$ , are calculated to be separated by a pronounced barrier. In our previous study [22], we have demonstrated that by allowing the rotational axis to tilt away from the PA, one of these minima becomes a saddle point, thus clarifying the nature of the TSD1 and TSD2 bands. In our fully self-consistent TAC Skyrme-HF (SHF) and HF-Bogoliubov (SHFB) calculations, we noticed that the KO conditions, which in the past have never been practically implemented in the EDF approaches, are numerically fulfilled with high precision. Here, we provide an in-depth analysis of these conditions and discuss their physical consequences.

The paper is organized as follows. In Sec. II, we present a re-derivation of the KO conditions and extend it to the framework of the Kohn-Sham (KS) theory, where one does not employ Hamiltonian but an EDF. Sec. III explains the model used in the present work and expresses the KO conditions in terms of conventions used by the HFODD solver. Section. IV contains the results of calculations. Finally, the conclusions of this work are given in Sec. V.

## II. KERMAN-ONISHI CONDITIONS

The conditions for a general nuclear rotation around arbitrary axis were proposed by Kerman and Onishi [11] within the time-dependent variational method. In the following Subsection, to fix the notation, we recall the original derivation that is based on the constrained HF method.

### A. Kerman-Onishi conditions in the Hartree-Fock approach with a Hamiltonian

Within the constrained HF method, the rotation is imposed by adding a cranking term,  $-\boldsymbol{\omega} \cdot \hat{\mathbf{J}}$  to the Hamiltonian  $\hat{H}$ , where  $\hat{\mathbf{J}}$  is the angular momentum operator and  $\boldsymbol{\omega}$  are three Lagrange multipliers identified with the rotational frequency vector. The intrinsic frame is defined by bringing the average values of the symmetric second-rank tensor,

$$\hat{Q}_{ij} \equiv x_i x_j, \quad (1)$$

to its PA. This can be achieved by requiring that the average values of three off-diagonal components of  $\hat{Q}_{ij}$ :

$$\hat{B}_k = \hat{Q}_{ij}, \quad (ijk; \text{cyclic}), \quad (2)$$

are zero in the HF state  $|\Phi\rangle$ :

$$\langle \Phi | \hat{\mathbf{B}} | \Phi \rangle = 0. \quad (3)$$

The resulting Routhian can be written as:

$$\hat{H}' = \hat{H} - \boldsymbol{\omega} \cdot \hat{\mathbf{J}} - \boldsymbol{\lambda} \cdot \hat{\mathbf{B}}, \quad (4)$$

where  $\boldsymbol{\lambda}$  are three Lagrange multipliers enforcing condition (3), and the rotational frequencies  $\boldsymbol{\omega}$  are determined from the angular-momentum condition:

$$\mathbf{J} = \langle \Phi | \hat{\mathbf{J}} | \Phi \rangle. \quad (5)$$

The original derivation of KO conditions is based on the fact that for the stationary HF state  $|\Phi\rangle$  that minimizes the Routhian

$$\delta \langle \Phi | \hat{H}' | \Phi \rangle = 0, \quad (6)$$

the following condition holds:

$$\langle \Phi | [\hat{H}', \hat{\mathbf{J}}] | \Phi \rangle = 0. \quad (7)$$

By assuming the rotational invariance of the Hamiltonian:

$$[\hat{H}, \hat{\mathbf{J}}] = 0, \quad (8)$$

denoting the three diagonal components of (1) as  $\hat{D}_i \equiv \hat{Q}_{ii}$ , and noticing that

$$\begin{aligned} [\hat{B}_i, \hat{J}_j] &= -i\hat{B}_k, \\ [\hat{B}_k, \hat{J}_k] &= i(\hat{D}_i - \hat{D}_j), \end{aligned} \quad (ijk; \text{cyclic}) \quad (9)$$

one arrives at the original KO conditions:

$$\lambda_k = \frac{(\boldsymbol{\omega} \times \mathbf{J})_k}{D_i - D_j} \quad (ijk; \text{cyclic}), \quad (10)$$

where  $D_i = \langle \Phi | \hat{D}_i | \Phi \rangle$ . Consequently, nonzero values of Lagrange multipliers  $\boldsymbol{\lambda}$  imply that vectors  $\boldsymbol{\omega}$  and  $\mathbf{J}$  are not parallel. We note here that  $\hat{B}_k$ ,  $\hat{D}_i$ , and  $\lambda_k$  are numbered by three Cartesian directions and thus we use for them the standard bold-face notations  $\hat{\mathbf{B}}$ ,  $\hat{\mathbf{D}}$ , and  $\boldsymbol{\lambda}$ , respectively; however, under space rotations they do not transform as vectors.

### B. Kerman-Onishi conditions in a DFT approach with an energy density functional

In the framework of the KS approach of the DFT [25], the basic entity is the energy density  $\mathcal{H}(\mathbf{r})$ , which gives the total binding energy of the system in terms of the one-body density matrix  $\rho$ :

$$E\{\rho\} = \int d^3\mathbf{r} \mathcal{H}(\mathbf{r}) = E_k\{\rho\} + E_p\{\rho\}, \quad (11)$$

expressed in terms of kinetic and potential energy terms. The minimization of  $E\{\rho\}$  with respect to  $\rho$  under conditions (3) and (5) results in self-consistent KS equations:

$$[h'(\rho), \rho] = 0, \quad (12)$$

where  $h' = h - \boldsymbol{\omega} \cdot \hat{\mathbf{J}} - \boldsymbol{\lambda} \cdot \hat{\mathbf{B}}$  and the mean-field Hamiltonian  $h$  is now given by the functional derivative of  $E\{\rho\}$ :

$$h = \frac{\partial}{\partial \rho} E\{\rho\} = t + \Gamma, \quad (13)$$

with  $t = \frac{\partial}{\partial \rho} E_k\{\rho\}$  being the one-body kinetic term and  $\Gamma = \frac{\partial}{\partial \rho} E_p\{\rho\}$  – one-body potential-energy term.

It is important to realize that in the KS approach, neither many-body Hamiltonian  $\hat{H}$  nor wave function  $|\Phi\rangle$  are well-defined entities, unless the energy density  $\mathcal{H}$  is explicitly derived from an effective two-body interaction [26]. Moreover, even if the actual approach is based on a Hamiltonian, the self-consistent density  $\rho$  and the potential term  $\Gamma(\rho)$  obtained from Eq. (12) usually break the original symmetries of  $\hat{H}$  (in particular the rotational invariance) due to the spontaneous symmetry breaking mechanism. Consequently, if  $\hat{H}$  depends on density, as in the case of Skyrme and Gogny interactions, condition (8) obviously does not hold.

Let us now consider the group SO(3) of rotations. The corresponding transformation is represented by the unitary operator  $\hat{R}(\boldsymbol{\theta}) = \exp(i\boldsymbol{\theta} \cdot \hat{\mathbf{J}})$ , where  $\boldsymbol{\theta}$  is a three-dimensional rotation vector. As discussed in Refs. [27, 28], since the energy density is covariant with  $\hat{R}(\boldsymbol{\theta})$ , that is,

$$\mathcal{H}^R(\mathbf{r}) = \mathcal{H}(\hat{R}^+ \mathbf{r} \hat{R}), \quad (14)$$

and the kinetic term is a scalar, the potential energy is invariant with respect to a unitary transformation of the density [29]

$$E_p(\rho) = E_p(\hat{R}\rho\hat{R}^+). \quad (15)$$

As a matter of fact, relation (15) applies not only to the total potential energy but also to individual contributions to  $E_p$  associated with terms characterized by different coupling constants. Physically, Eq. (15) simply means that the total energy does not depend on the orientation of the intrinsic density in space.

The first-order expansion in  $\boldsymbol{\theta}$  yields [29]

$$E_p(\hat{R}\rho\hat{R}^+) = E_p(\rho) + i\boldsymbol{\theta} \cdot \text{Tr}(\Gamma[\hat{\mathbf{J}}, \rho]). \quad (16)$$

Consequently,

$$\text{Tr}(\Gamma[\hat{\mathbf{J}}, \rho]) = \text{Tr}(\rho[\Gamma, \hat{\mathbf{J}}]) = \langle [\Gamma, \hat{\mathbf{J}}] \rangle = 0, \quad (17)$$

where the symbol  $\langle \dots \rangle$  means an average value  $\text{Tr}(\rho \dots)$ . A KS analog of the Hamiltonian expression (7) can be written as

$$\text{Tr}(\rho[h', \hat{\mathbf{J}}]) = \text{Tr}(\hat{\mathbf{J}}[\rho, h']) = 0, \quad (18)$$

where we used the self-consistency condition (12). Finally, by combining (17) and (18) we obtain

$$\langle [\boldsymbol{\omega} \cdot \hat{\mathbf{J}} + \boldsymbol{\lambda} \cdot \hat{\mathbf{B}}, \hat{\mathbf{J}}] \rangle = 0, \quad (19)$$

which, with the help of (9), yields the KO conditions (10) in the KS case, with  $\langle \Phi | \dots | \Phi \rangle$  being replaced by  $\text{Tr}(\rho \dots)$ .

The extension to superfluid DFT, or self-consistent Hartree-Fock-Bogoliubov (HFB) theory is straightforward: in the derivations above, the single-particle density

matrix  $\rho$  is replaced by the generalized  $2 \times 2$  density matrix  $\mathcal{R}$ , also involving the abnormal (pair) density  $\tilde{\rho}$  [30], and the mean-field  $h$  is replaced by the  $2 \times 2$  HFB Hamiltonian, containing the pairing field  $\tilde{h}$ . All other steps are identical; one needs to remember that the one-body operators  $\hat{\mathbf{B}}$  and  $\hat{\mathbf{J}}$  act only in the particle-hole space, that is, the average values do not involve the abnormal density.

### III. THE MODEL

In this work, all calculations were performed by using the symmetry-unrestricted solver HFODD (version 2.49t) [31]. For tests of KO conditions in  $^{158}\text{Er}$  and TAC calculations of TSD bands in  $^{160}\text{Yb}$ , we performed the SHF calculation without pairing. We used the Skyrme EDF SkM\* [32] and 1,000 deformed harmonic-oscillator (HO) basis states with HO frequencies of  $\hbar\Omega_x = \hbar\Omega_y = 10.080\text{MeV}$  (up to  $N_x = N_y = 15$  HO quanta) and  $\hbar\Omega_z = 7.418\text{MeV}$  (up to  $N_z = 20$  HO quanta). Detailed tests show that such a size of the basis provides us with a sufficient precision for the quantities studied in this work. Tests of the KO conditions in  $^{158}\text{Er}$  were performed at rotational frequency of  $\hbar\omega = 0.6\text{MeV}$  and for configuration denoted by  $\nu[23, 23, 22, 22] \otimes \pi[17, 18, 16, 17]$ . The configurations are labeled by the numbers of states occupied in the four parity-signature  $(\pi, r)$  blocks, in the convention of Ref. [33].

Technically, these numbers correspond to the conserved  $x_2$ -signature, and thus are valid only for rotations around the  $x_2$  axis. However, for a two-dimensional cranking tilted within a symmetry plane of the matter distribution, the  $\mathbf{J}$ -signature corresponding to the direction of the angular-momentum vector remains a good quantum number for any tilting angle  $\theta$ . Therefore, the given numbers of states can be understood as pertaining to the  $\mathbf{J}$ -signature. Of course, for non-zero tilting angles, the code must be run in the broken- $x_2$ -signature mode, whereupon the configurations are set by fixing numbers of states occupied in parity blocks only.

To check the KO conditions in the presence of pairing, we also performed TAC HFB calculations for  $^{110}\text{Mo}$ , with Lipkin-Nogami pairing (HFB+LN) included [33]. The neutron and proton pairing strengths were chosen as  $(V_0^\nu, V_0^\pi) = (-196, -218)\text{MeV}$ , with a cutoff energy in the quasiparticle spectrum of  $E_{\text{cut}} = 60\text{MeV}$ . This choice of the specific nucleus and pairing strengths was dictated by the fact that with this choice one obtains a well defined triaxial solution with sizable pairing, which makes it a very suitable test case for the KO conditions in HFB.

To link Eq. (10) to total quadrupole moments of the nucleus, we first rewrite it terms of spherical components of the quadrupole tensor (1). In the HFODD convention for multipole moments, we have:

$$Q_{\lambda\mu}(\mathbf{r}) = a_{\lambda\mu} r^\lambda Y_{\lambda\mu}^*(\theta, \phi), \quad (20)$$

where  $Y_{\lambda\mu}$  are the standard spherical harmonics in the

convention of Ref. [34] and normalization factors  $a_{\lambda\mu}$  have been defined in Table 5 of Ref. [33]. Then we have explicitly,

$$Q_{20} = 2x_3^2 - x_1^2 - x_2^2, \quad (21a)$$

$$Q_{21} = x_3x_1 - ix_3x_2, \quad (21b)$$

$$Q_{22} = \sqrt{3}(x_1^2 - x_2^2 - 2ix_1x_2), \quad (21c)$$

with  $Q_{2-1} = -Q_{21}^*$  and  $Q_{2-2} = Q_{22}^*$ , and thus,

$$x_1x_2 = \frac{\sqrt{3}}{6}\Im Q_{2-2}, \quad (22)$$

$$x_1x_3 = \Re Q_{21}, \quad (23)$$

$$x_2x_3 = \Im Q_{2-1}, \quad (24)$$

$$x_1^2 - x_2^2 = \frac{\sqrt{3}}{3}\Re Q_{22}, \quad (25)$$

$$x_3^2 - x_2^2 = \frac{\sqrt{3}}{6}\Re Q_{22} + \frac{1}{2}Q_{20}, \quad (26)$$

$$x_3^2 - x_1^2 = -\frac{\sqrt{3}}{6}\Re Q_{22} + \frac{1}{2}Q_{20}. \quad (27)$$

By means of Eqs. (22)-(27), the KO conditions (10) read:

$$\begin{aligned} -\lambda_1x_2x_3 &= +\frac{\omega_2j_3 - \omega_3j_2}{\frac{\sqrt{3}}{6}\Re\langle Q_{22}\rangle + \frac{1}{2}\langle Q_{20}\rangle}\Im Q_{2-1} \\ &\equiv -L'_{2-1}\Im Q_{2-1}, \end{aligned} \quad (28a)$$

$$\begin{aligned} -\lambda_2x_1x_3 &= -\frac{\omega_3j_1 - \omega_1j_3}{-\frac{\sqrt{3}}{6}\Re\langle Q_{22}\rangle + \frac{1}{2}\langle Q_{20}\rangle}\Re Q_{21} \\ &\equiv -L'_{21}\Re Q_{21}, \end{aligned} \quad (28b)$$

$$\begin{aligned} -\lambda_3x_1x_2 &= -\frac{\omega_1j_2 - \omega_2j_1}{2\Re\langle Q_{22}\rangle}\Im Q_{2-2} \\ &\equiv -L'_{2-2}\Im Q_{2-2}, \end{aligned} \quad (28c)$$

which can be conveniently written in terms of factors  $L'_{2-1}$ ,  $L'_{21}$ , and  $L'_{2-2}$ .

Following Ref. [22], in the calculations presented in this study we only allow the rotational axis to tilt from the  $x_2$ -axis into the  $x_1$ - $x_2$  plane; that is, the cranking is two dimensional. In this case, only one of the three constraints,  $-L_{2-2}\Im Q_{2-2}$ , is active. The other two constraints,  $\langle\Im Q_{2-1}\rangle = 0$  and  $\langle\Re Q_{21}\rangle = 0$ , are automatically realized by enforcing the  $x_3$ - $T$ -simplex symmetry [35]. Then, in each iteration,  $L_{2-2}$  is updated so as to guarantee that  $\langle Q_{2-2}\rangle = 0$ . To obtain a precise value of this constraint, we use the augmented Lagrange method [36]. Upon convergence, one obtains values of  $L_{2-2}$ , components of total angular momentum,  $j_1$  and  $j_2$ , and  $\langle Q_{22}\rangle$ . Inserting  $j_1$ ,  $j_2$ , and  $\langle Q_{22}\rangle$  into relation (28c), one obtains values of  $L'_{2-2} = \frac{\omega_1j_2 - \omega_2j_1}{2\Re\langle Q_{22}\rangle}$ . By comparing  $L_{2-2}$  and  $L'_{2-2}$  one can assess the extent the KO conditions are fulfilled.

## IV. RESULTS

### A. Tests of the Kerman-Onishi conditions

Figure 1 displays values of  $L_{2-2}/L'_{2-2}$ , calculated for the triaxial bands in  $^{158}\text{Er}$  and  $^{110}\text{Mo}$  defined in Sec. III, as a function of the tilting angle  $\theta$  in the  $x_1$ - $x_2$  plane. The quantity  $L_{2-2}$  is obtained from the self-consistent SHF (SHFB+LN) calculations, and  $L'_{2-2}$  is obtained by means of Eq. (28c). It can be seen that for the most of values of  $\theta$ , ratios  $L_{2-2}/L'_{2-2}$  stay inside the interval of [0.999-1.001], which means the first 3 significant digits of  $L_{2-2}$  and  $L'_{2-2}$  are the same. We can thus see that in our HF and HFB calculations the KO conditions are fulfilled with a rather high precision. We note that at  $\theta = 0$  or  $90^\circ$ , the solutions correspond to the uniform PA rotation, and thus the values of both  $L_{2-2}$  and  $L'_{2-2}$  tend to zero; hence, the ratios  $L_{2-2}/L'_{2-2}$  cannot be determined.

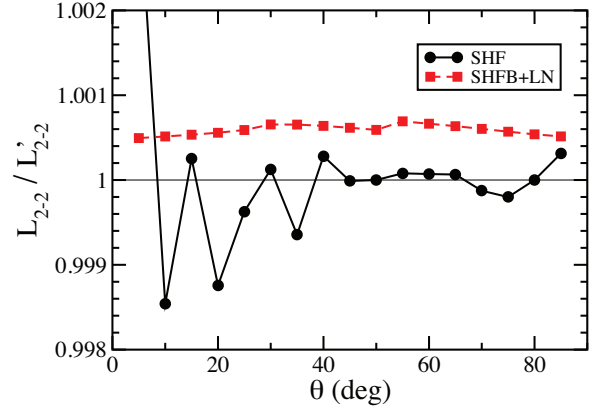


FIG. 1. (Color online) The  $L_{2-2}/L'_{2-2}$  ratio for a TSD band in  $^{158}\text{Er}$  (SHF) and a triaxial band in  $^{110}\text{Mo}$  (SHFB+LN) as a function of the tilting angle  $\theta$  defined in the  $x_1$ - $x_2$  plane. The quantity  $L_{2-2}$  is obtained self-consistently while  $L'_{2-2}$  is defined through Eq. (28c).

The energetics governing TAC rotations is illustrated in Fig. 2, which shows energies, Routhians,  $L_{2-2}$ , and the angle  $\alpha$  between  $\boldsymbol{\omega}$  and  $\boldsymbol{J}$  as functions of  $\theta$  for  $^{158}\text{Er}$  and  $^{110}\text{Mo}$ . It is seen that in these two triaxially deformed systems, stationary solutions appear only at  $\theta = 0^\circ$  or  $90^\circ$ . The value of  $L_{2-2}$  vanishes at stationary points, and it becomes finite when the Routhian has a nonzero slope as a function of  $\theta$ . The value of angle  $\alpha$  always remains fairly small, in  $^{158}\text{Er}$  and  $^{110}\text{Mo}$  reaching  $0.1$  and  $1^\circ$ , respectively.

As seen in Fig. 1, there appear small residual deviations between  $L_{2-2}$  and  $L'_{2-2}$  that need to be understood. To this end, in Fig. 3 we show the ratio  $L_{2-2}/L'_{2-2}$  calculated at  $\theta = 40^\circ$  as a function of the number of iterations. We see that in the SHF case the convergence of the ratio to the exact value of  $L_{2-2}/L'_{2-2} = 1$  can be slow. Because of that, by stopping the iteration when the convergence at every  $\theta$  reaches a fixed stability, one obtains

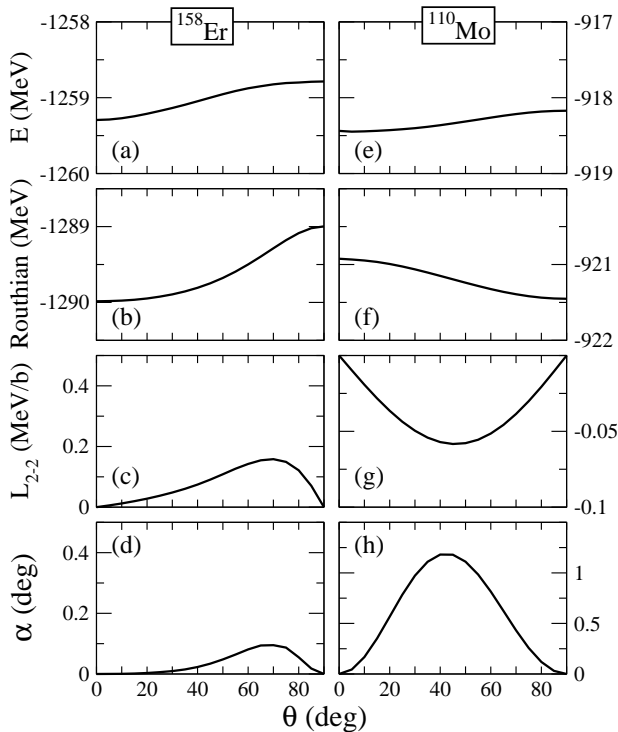


FIG. 2. From top to bottom: energies, Routhians,  $L_{2-2}$ , and  $\alpha$  (angle between  $\omega$  and  $\mathbf{J}$ ) as functions of the tilting angle  $\theta$  for triaxial bands in  $^{158}\text{Er}$  (left) and  $^{110}\text{Mo}$  (right).

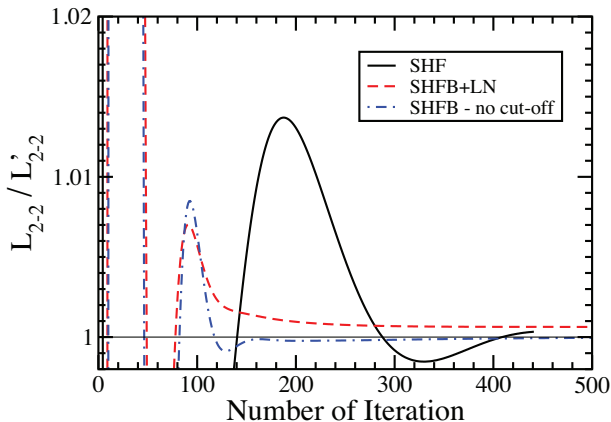


FIG. 3. (Color online) The ratio  $L_{2-2}/L'_{2-2}$  as a function of iteration number at  $\theta = 40^\circ$  for SHF, SHFB+LN, and SHFB (no cut-off). See text for details.

values of  $L_{2-2}/L'_{2-2}$  that differ from one by small residuals that vary from point to point.

For the SHFB+LN calculations, the convergence pattern is entirely different. Here, the ratios of  $L_{2-2}/L'_{2-2}$  rapidly converge, but the obtained limit systematically deviates from one by a small number  $\approx 0.0006$ . It turns out that this result can be attributed to the truncation of the quasiparticle spectrum, which is routinely employed in the HFB calculations when dealing with zero-range

pairing interactions. Indeed, such truncation makes the pairing tensor acquire a small symmetric part, which is bosonic in character [37, 38]. When we switch off the LN procedure and increase the cutoff energy  $E_{\text{cut}}$  in such a way that the variational method is rigorously valid and all quasiparticles are included, values of  $L_{2-2}/L'_{2-2}$  converge perfectly to one as one can assess from Fig. 3.

To conclude, small deviations from the exact limit of  $L_{2-2}/L'_{2-2} = 1$  seen in Fig. 1 are very well understood, and the KO conditions can be, in fact, met to an arbitrary precision. Of course, in practical calculations aiming at a determination of nuclear observables, the precision slightly below 0.01% is perfectly sufficient.

### B. Tilted-axis- cranking calculations for triaxial strongly deformed bands in $^{160}\text{Yb}$

As an illustrative example of our SHF calculations, in this section we present results obtained for predicted TSD bands in  $^{160}\text{Yb}$ . A good indicator of unstable PAC solutions is the appearance of competing PAC minima with similar values of  $\beta_2$  and  $|\gamma|$  but opposite values of  $\gamma$ , as discussed in Sec. I. Therefore, before computing the Routhians as functions of the tilting angle, we first performed extensive PAC calculations so as to determine deformations of various minima. Similar to the PAC calculations in  $^{158}\text{Er}$  [24], we found that the configurations generally have three typical deformations, namely,  $(Q_t, \gamma) \sim (9\text{ eb}, 9^\circ\text{--}14^\circ)$  (TSD1),  $(Q_t, \gamma) \sim (12.2\text{--}10.8\text{ eb}, -10^\circ)$  (TSD2), and  $(Q_t, \gamma) \sim (10.0\text{--}10.5\text{ eb}, 13^\circ)$  (TSD3). Ranges of deformations indicate shape changes with rotational frequency.

TABLE I. The configurations in  $^{160}\text{Yb}$  studied in this work. Each configuration is described by the numbers of states occupied in the four parity-signature  $(\pi, r)$  blocks, in the convention of Ref. [33].

Label	minimum	Configuration	parity
A	TSD1	$\nu[23, 23, 22, 22] \otimes \pi[16, 18, 18, 18]$	+
B	TSD1	$\nu[23, 24, 21, 22] \otimes \pi[16, 18, 18, 18]$	-
C	TSD1	$\nu[23, 24, 21, 22] \otimes \pi[18, 18, 17, 17]$	-
D	TSD3	$\nu[23, 23, 22, 22] \otimes \pi[18, 18, 17, 17]$	+
E	TSD3	$\nu[23, 23, 22, 22] \otimes \pi[17, 17, 18, 18]$	+

Figure 4 shows total Routhians of five configurations in  $^{160}\text{Yb}$  calculated in SHFB+LN as functions of  $\theta$ . The corresponding configurations and parities are given in Table I. At  $\theta = 90^\circ$ , the  $Q_{22}$  value changes sign and TSD1 becomes TSD2. It can be seen that at rotational frequency  $\omega = 0.5\text{ MeV}$ , the Routhians of the lowest bands A and B are very soft against  $\theta$ . Interestingly, for the configuration A, a minimum at  $\theta \neq 0$  or  $90^\circ$  develops. In such a situation, one may expect the large-amplitude collective motion of the rotational axis along  $\theta$ . The energies of bands TSD2 rapidly increase with  $\omega$ , and these configurations become saddle points. For the frequencies

considered, the two lowest TSD3 configurations are close in energy to, or even below, the TSD1 and TSD2 bands.

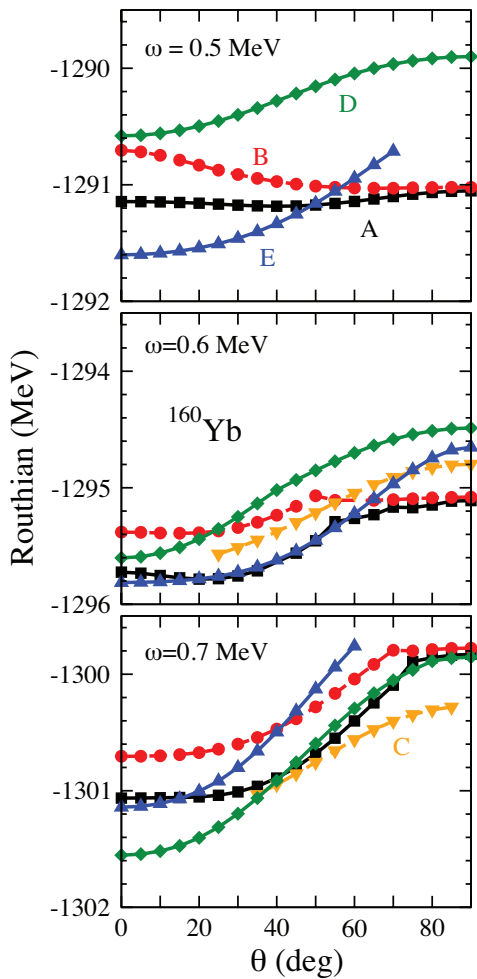


FIG. 4. (Color online) Total Routhians in  $^{160}\text{Yb}$  calculated within the SHF method as functions of the tilting angle  $\theta$  for the five TSD configurations listed in Table I. Solid and dashed lines mark configurations with positive and negative parity, respectively.

## V. CONCLUSIONS

In this study we re-examined the Kerman-Onishi conditions for a triaxial quantum rotation within the self-consistent Kohn-Sham theory. We first derived the KO equations without invoking the concept of Hamiltonian or wave function but rather in terms of energy density functional and nucleonic densities. Not surprisingly, the final form of the KO condition (10) is the same as that originally derived for the HF approximation.

In the next step, we performed numerical tests of the KO condition within the SHF and SHFB+LN methods. For the first time, these relations have been tested in a fully self-consistent EDF approach, including pairing. By comparing the self-consistently obtained Lagrange multiplier  $L_{2-2}$  with the value  $L'_{2-2}$  given by Eq. (10), we demonstrated that in our TAC calculations, the KO conditions are fulfilled to a very high precision. We noticed that when differences between  $L_{2-2}$  and  $L'_{2-2}$  occur, those are excellent indicators of the variational principle violations due to practical approximations (such as, e.g., the quasiparticle basis truncation in HFB).

Finally, we performed 2D TAC calculations for the low-lying TSD bands in  $^{160}\text{Yb}$ . At lower frequencies, we predict rather  $\theta$ -soft Routhian curves, indicative of the large-amplitude collective motion. With increasing rotational frequency, TSD1 configurations become favored energetically and TSD2 represent unphysical saddle points. TSD3 configurations become lower in energy than those of TSD1 and TSD2 configurations already at  $\omega \approx 0.5$  MeV, which is much lower than what has been predicted for  $^{158}\text{Er}$ . A detailed analysis of TSD bands in  $^{160}\text{Yb}$  will be published elsewhere.

In summary, over thirty years ago, kinematic conditions for a quantum rotation of triaxial nuclei were derived within the self-consistent theory. Now, for the first time, we have performed EDF calculations that strictly obey those conditions. Our results are significant for several reasons. First, they answer a long-standing question in nuclear physics by showing that the rotations around the axes in a deformed nucleus are not independent of one another. The advent of computational tools has provided the ample numerical power to make the numerical calculations of self-consistent TAC rotations possible. Second, such calculations are essential for interpreting TSD bands seen experimentally. Finally, we demonstrated the existence of rotational bands that are  $\theta$ -soft, that is, for which the tilting angle cannot be defined. To understand such structures will require going beyond the single-reference DFT.

## ACKNOWLEDGMENTS

We thank J.A. Sheikh for useful discussions. This work was supported by the U.S. Department of Energy (DOE) under Contracts No. DE-FG02-96ER40963 (University of Tennessee), No. de-sc0008499 (NUCLEI SciDAC Collaboration), Academy of Finland and University of Jyväskylä within the FIDIPRO programme, and Polish National Science Center under Contract No. 2012/07/B/ST2/03907.

[1] P. Ring and P. Schuck, *The Nuclear Many-body Problem* (Springer-Verlag, Heidelberg, 1980).

[2] Z. Szymański, *Fast Nuclear Rotation* (Clarendon Press,

- Oxford, 1983).
- [3] M. J. A. de Voigt, J. Dudek, and Z. Szymański, *Rev. Mod. Phys.* **55**, 949 (1983).
- [4] D. R. Inglis, *Phys. Rev.* **96**, 1059 (1954).
- [5] S. Frauendorf, *Rev. Mod. Phys.* **73**, 463 (2001).
- [6] S. Frauendorf and J. Meng, *Nucl. Phys. A* **617**, 131 (1997).
- [7] P. Möller, R. Bengtsson, B. Carlsson, P. Olivius, T. Ichikawa, H. Sagawa, and A. Iwamoto, *At. Data Nucl. Data Tables* **94**, 758 (2008).
- [8] J. Snyder *et al.*, *Phys. Lett. B* **723**, 61 (2013).
- [9] H. Frisk and R. Bengtsson, *Phys. Lett. B* **196**, 14 (1987).
- [10] W. Nazarewicz and I. Ragnarsson, in *Handbook of Nuclear Properties*, edited by D. Poenaru and W. Greiner (Oxford Science Publications, Clarendon Press, Oxford, 1996) p. 80.
- [11] A. Kerman and N. Onishi, *Nucl. Phys. A* **361**, 179 (1981).
- [12] W. Nazarewicz and Z. Szymański, *Phys. Rev. C* **45**, 2771 (1992).
- [13] T. Horibata and N. Onishi, *Nucl. Phys. A* **596**, 251 (1996); M. Oi, N. Onishi, N. Tajima, and T. Horibata, *Phys. Lett. B* **418**, 1 (1998); M. Oi and P. M. Walker, *ibid.* **576**, 75 (2003).
- [14] E. S. Paul, P. J. Twin, A. O. Evans, A. Pipidis, M. A. Riley, J. Simpson, D. E. Appelbe, D. B. Campbell, P. T. W. Choy, R. M. Clark, M. Cromaz, P. Fallon, A. Gørgen, D. T. Joss, I. Y. Lee, A. O. Macchiavelli, P. J. Nolan, D. Ward, and I. Ragnarsson, *Phys. Rev. Lett.* **98**, 012501 (2007).
- [15] N. Pattabiraman, Y. Gu, S. Frauendorf, U. Garg, T. Li, B. Nayak, X. Wang, S. Zhu, S. Ghugre, R. Janssens, R. Chakrawarthy, M. Whitehead, and A. Macchiavelli, *Phys. Lett. B* **647**, 243 (2007).
- [16] A. Aguilar, D. B. Campbell, K. Chandler, A. Pipidis, M. A. Riley, C. Teal, J. Simpson, D. J. Hartley, F. G. Kondev, R. M. Clark, M. Cromaz, P. Fallon, I. Y. Lee, A. O. Macchiavelli, and I. Ragnarsson, *Phys. Rev. C* **77**, 021302 (2008).
- [17] C. Teal, K. Lagergren, A. Aguilar, D. J. Hartley, M. A. Riley, J. Simpson, M. P. Carpenter, U. Garg, R. V. F. Janssens, D. T. Joss, F. G. Kondev, T. Lauritsen, C. J. Lister, X. Wang, S. Zhu, and I. Ragnarsson, *Phys. Rev. C* **78**, 017305 (2008).
- [18] J. Ollier, J. Simpson, X. Wang, M. A. Riley, A. Aguilar, C. Teal, E. S. Paul, P. J. Nolan, M. Petri, S. V. Rigby, J. Thomson, C. Unsworth, M. P. Carpenter, R. V. F. Janssens, F. G. Kondev, T. Lauritsen, S. Zhu, D. J. Hartley, I. G. Darby, and I. Ragnarsson, *Phys. Rev. C* **80**, 064322 (2009).
- [19] J. Ollier, J. Simpson, M. Riley, E. Paul, X. Wang, A. Aguilar, M. Carpenter, I. Darby, D. Hartley, R. F. Janssens, F. Kondev, T. Lauritsen, P. Nolan, M. Petri, J. Rees, S. Rigby, C. Teal, J. Thomson, C. Unsworth, S. Zhu, A. Kardan, and I. Ragnarsson, *Phys. Rev. C* **83**, 044309 (2011).
- [20] X. Wang, M. Riley, J. Simpson, E. Paul, J. Ollier, R. Janssens, A. Ayangeakaa, H. Boston, M. Carpenter, C. Chiara, U. Garg, D. Hartley, D. Judson, F. Kondev, T. Lauritsen, N. Lumley, J. Matta, P. Nolan, M. Petri, J. Revill, L. Riedinger, S. Rigby, C. Unsworth, S. Zhu, and I. Ragnarsson, *Phys. Lett. B* **702**, 127 (2011).
- [21] J. Dudek and W. Nazarewicz, *Phys. Rev. C* **31**, 298 (1985).
- [22] Y. Shi, J. Dobaczewski, S. Frauendorf, W. Nazarewicz, J. C. Pei, F. R. Xu, and N. Nikolov, *Phys. Rev. Lett.* **108**, 092501 (2012).
- [23] A. Kardan, I. Ragnarsson, H. Miri-Hakimabad, and L. Rafat-Motevali, *Phys. Rev. C* **86**, 014309 (2012).
- [24] A. V. Afanasjev, Y. Shi, and W. Nazarewicz, *Phys. Rev. C* **86**, 031304 (2012).
- [25] W. Kohn and L. J. Sham, *Phys. Rev.* **140**, A1133 (1965).
- [26] M. Bender, P.-H. Heenen, and P.-G. Reinhard, *Rev. Mod. Phys.* **75**, 121 (2003).
- [27] B. G. Carlsson, J. Dobaczewski, and M. Kortelainen, *Phys. Rev. C* **78**, 044326 (2008).
- [28] S. G. Rohoziński, J. Dobaczewski, and W. Nazarewicz, *Phys. Rev. C* **81**, 014313 (2010).
- [29] F. Raimondi, B. G. Carlsson, J. Dobaczewski, and J. Toivanen, *Phys. Rev. C* **84**, 064303 (2011).
- [30] J. Dobaczewski, H. Flocard, and J. Treiner, *Nucl. Phys. A* **422**, 103 (1984).
- [31] N. Schunck, J. Dobaczewski, J. McDonnell, W. Satuła, J. Sheikh, A. Staszczak, M. Stoitsov, and P. Toivanen, *Comput. Phys. Commun.* **183**, 166 (2012).
- [32] J. Bartel, P. Quentin, M. Brack, C. Guet, and H.-B. Håkansson, *Nucl. Phys. A* **386**, 79 (1982).
- [33] J. Dobaczewski and P. Olbratowski, *Comput. Phys. Commun.* **158**, 158 (2004).
- [34] D. Varshalovitch, A. Moskalev, and V. Kersonskii, *Quantum Theory of Angular Momentum* (World Scientific, Singapore, 1988).
- [35] J. Dobaczewski, J. Dudek, S. Rohoziński, and T. Werner, *Phys. Rev. C* **62**, 014310 (2000).
- [36] A. Staszczak, M. Stoitsov, A. Baran, and W. Nazarewicz, *Eur. Phys. J. A* **46**, 85 (2010).
- [37] J. Dobaczewski, P. Borycki, W. Nazarewicz, and M. Stoitsov, *Eur. Phys. J. A* **25**, s1.541 (2005).
- [38] J. Dobaczewski and W. Nazarewicz, in *50 Years of Nuclear BCS*, edited by R. A. Broglia and V. Zelevinski (World Scientific, 2012) pp. 40–60.